

An olfactory cocktail party: figure-ground segregation of odorants in rodents

Dan Rokni^{1,2}, Vivian Hemmelder^{1,2}, Vikrant Kapoor^{1,2} & Venkatesh N Murthy^{1,2}

In odorant-rich environments, animals must be able to detect specific odorants of interest against variable backgrounds. However, studies have found that both humans and rodents are poor at analyzing the components of odorant mixtures, suggesting that olfaction is a synthetic sense in which mixtures are perceived holistically. We found that mice could be easily trained to detect target odorants embedded in unpredictable and variable mixtures. To relate the behavioral performance to neural representation, we imaged the responses of olfactory bulb glomeruli to individual odors in mice expressing the Ca^{2+} indicator GCaMP3 in olfactory receptor neurons. The difficulty of segregating the target from the background depended strongly on the extent of overlap between the glomerular responses to target and background odors. Our study indicates that the olfactory system has powerful analytic abilities that are constrained by the limits of combinatorial neural representation of odorants at the level of the olfactory receptors.

Rodents, like many other animals, rely on olfaction for their survival. It is the primary sense for finding food and mates and avoiding predators^{1–3}. As natural environments are rich in stimuli from multiple and variable sources, identifying any stimulus of interest necessitates segregating it from the background. Scene analysis and segmentation have been studied extensively in vision^{4,5} and audition^{6,7}, but very little is known about analysis of odorous scenes^{8,9}. Indeed, while contemporary studies in vision and audition focus on the mechanisms underlying scene segmentation, even the mere behavioral ability continues to be questioned for olfaction^{9–11}.

The difficulty of a complete analysis of an olfactory scene may arise from overlapping representations of odorants in the olfactory bulb. Odorant identity is thought to be combinatorially encoded in the olfactory bulb by the identity of activated receptors and their associated glomeruli^{12,13}. Each receptor can bind multiple odorants and a single odorant can bind multiple receptors. It follows that different odorants will elicit responses that are overlapping in glomerular space, eventually limiting the number of odorants that can be simultaneously encoded^{12,14}. Indeed, several studies have suggested that the olfactory system has a very limited capacity to encode multiple odorants simultaneously^{15–18} or even to detect a specific target odor within a mixture^{8,9,19–21}, unless odors are dispersed in time^{16,22}. These studies have contributed to the widely held view that olfaction is primarily a synthetic sense in which odorant mixtures elicit emergent perceptions at the expense of perceiving the individual components of the mixture^{10,11,22,23}.

Here we describe a behavioral task that directly tests the ability of mice to detect target stimuli within variable and unpredictable backgrounds. We further describe the relationship between the glomerular patterns of activity evoked by target and background odorants and the difficulty of segregating them.

RESULTS

Mice can segregate odorants from a background

We designed a behavioral task to answer two questions: (i) how does target detection depend on the number of background odorants? and (ii) how does target detection depend on the similarity between the target and the background odorants? Previous experiments in rodents have used fixed mixtures over many trials^{21,24} or temporally jittered binary mixtures^{25,26} to study object-background segregation. Here we randomly varied background odors, so that odor stimuli in different trials were rarely similar to each other. Additionally, unlike in earlier studies, head restraint allowed us to use well-controlled and timed stimuli, monitor responses more precisely and obtain thousands of trials.

Mice were trained on a Go/NoGo task in which they had to detect a target odorant within a mixture of odorants (**Fig. 1**), delivered through a custom-built olfactometer (**Supplementary Fig. 1**). Mice reported the presence of the target odorant (Go trial) by licking a water spout in front of their mouth and reported the absence of the target odorant from the mixture (NoGo trial) by refraining from licking. A correct lick was rewarded by a water drop and an incorrect trial was punished by a 5 s timeout.

Odorant mixtures were chosen from a pool of 16 odorants (**Fig. 2**) with varying degrees of similarity: 8 of the odorants contained a common functional group, tiglate (2-methylbut-2-enoate). Two of the 16 odorants were designated as targets and 14 were background for each mouse. The two target odorants were never presented together, the number of odorants in the mixture was limited to 14, and the probability of any target odorant being present in any single trial was kept constant at 0.5. These constraints yielded a total of 49,149 possible mixtures (rather than 65,536 without constraints). The use of 2 target odorants for each mouse reduced the risk of obtaining results that were highly dependent on the specific target. Furthermore,

¹Center for Brain Science, Harvard University, Cambridge, Massachusetts, USA. ²Department of Molecular & Cellular Biology, Harvard University, Cambridge, Massachusetts, USA. Correspondence should be addressed to V.N.M. (vnmurthy@fas.harvard.edu).

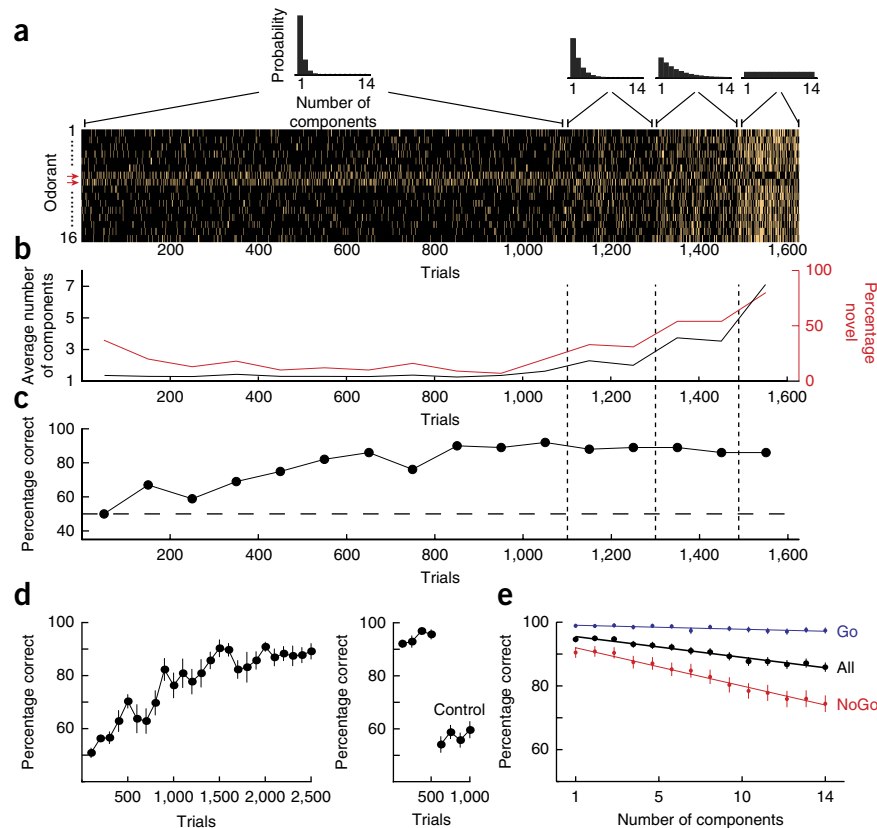
Received 13 February; accepted 3 July; published online 3 August 2014; doi:10.1038/nn.3775

Figure 1 The behavioral task. (a) The mixtures presented to one mouse during the first seven training sessions. Each row in the raster (bright ticks indicate presence of odorant) represents a single odorant and each column represents a trial. Odorants 7 and 8 were the targets for this mouse (red arrows to left). Above are the distributions of the number of components in the mixture used at each stage of the training. (b) The average number of components in the mixture in each 100 trial block (black) and the percentage of mixtures that the mouse was encountering for the first time (red). (c) The percent of correct trials in each 100-trial block. (d) Left, the average learning curve of 10 mice. Right, the last 400 trials performed with odorant cues and the first 400 trials performed when the target odorant tube was replaced with an empty tube or with a background odorant tube. Both plots show the mean \pm s.e.m. in 100-trial blocks. (e) Percentage of correct trials as a function of the number of components in the mixture for all trials (black), Go trials (blue), and NoGo trials (red). Symbols represent the mean and error bars show a 95% confidence interval. Lines are linear fits to the data.

to avoid obtaining odorant-specific results, we trained 13 mice on 8 different target pairs, with every odorant being the target for at least one mouse. Mice were first trained with mixtures that had few odorants until they reached 80% performance, and the distribution of the number of components in the mixture was then gradually adjusted to become uniform, where the probability of different numbers of odorants in the mixture was equal (Fig. 1a–c; see Online Methods). Mice typically reached criterion level performance (80%) within 1,000 trials (Fig. 1c,d). When the target odorant tubes were replaced with empty tubes or switched with background odorants, while keeping reward dependent on the same olfactometer channel where the target odorant used to be, performance dropped to near chance levels, confirming that mice were using odors as cues for performing the task (Fig. 1d). Notably, mice performed well on novel mixtures in the asymptotic phase (trial novelty rate of >60%; Fig. 1b), indicating an understanding of the task rules as opposed to learning of specific mixture–response associations.

We analyzed 30,400 trials performed by 13 mice in sessions after learning had reached a plateau and where the number of components in the mixture had a flat probability distribution. The first key result from our experiments is that mice performed well above chance level on mixtures with any number of odorant components, starting at 94% for 1 component and declining to 85% for 14 components (Fig. 1e). Each additional mixture component reduced performance by an average of 0.75%. These data indicate that mice are capable of performing olfactory figure-ground segregation and that performance degrades steadily with increasing number of background odorants.

The reduced performance for mixtures with more odorant components may reflect a greater degree of overlap in the neural representation of target and background odorants. Additionally, more difficult olfactory discriminations may require longer sampling for a decision to be made^{27,28}. Perhaps if mice were allowed longer sampling, performance would not degrade with the number of mixture components. Several findings argue against a limitation in sampling time as the explanation for reduced performance. First, mice were allowed 2 s to make a decision, and yet over 98% of licks had a latency of less than



1 s (Fig. 3a). Second, response latency was only weakly dependent on the number of odorants in the mixture (mean raw latency increased by 1.2 ms per added component—less than 0.25% of the mean; correlation coefficient 0.7; $P = 0.004$; Fig. 3b, top)^{29,30}. And third, the latencies at which asymptotic performance was reached were very similar in mixtures with different numbers of odorant components: that is, the benefit of longer sampling was similar for mixtures with either many components or just a few (Fig. 3c,d). These results indicate that the difficulty of solving the task does not arise from a sampling time limit, but probably reflects an actual overlap in the neural representation of the mixture components.

Effects of figure and background composition

In sensory systems operating in a well-defined stimulus space, such as vision and audition, the difficulty of figure-ground segregation depends on the similarity between features of the figure and the background. Whether a similar dependence exists in the olfactory system has been tested using binary odor mixtures and indirect measures of recognition such as odor investigation time^{21,31}. To test this hypothesis more directly, we analyzed separately trials from mice that were trained to detect tiglate targets ($n = 8$ mice) and trials from mice that were trained to detect non-tiglate targets ($n = 5$ mice). The logic was that tiglate targets (molecules containing the tiglate functional group) would have more similar odors in the background (other tiglates) than non-tiglate targets. Although chemical similarity does not necessarily imply perceptual similarity (discussed below), this analysis provides a link between the behavioral difficulty of figure-background segregation and the chemical features of the target and the background. In an analysis of 19,300 trials performed by 8 mice that were trained on tiglate targets (Fig. 4a) and 11,100 trials performed by 5 mice trained to detect non-tiglate targets (Fig. 4b) (analysis of individual mice is shown in Supplementary Figs. 2 and 3), performance dropped

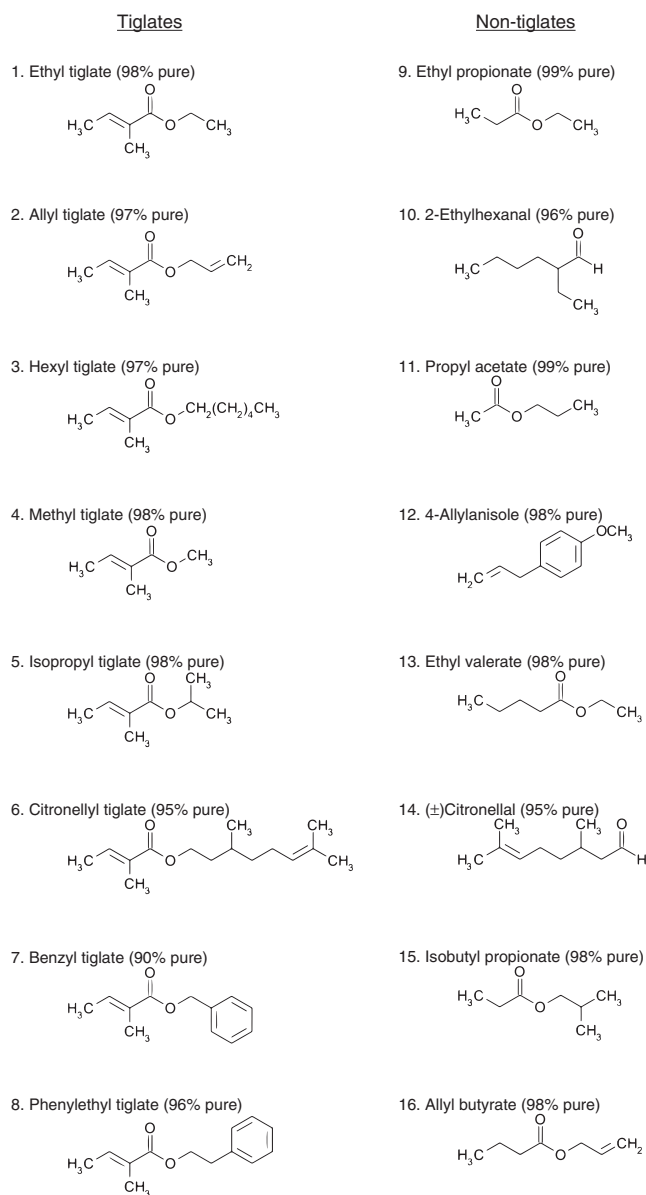


Figure 2 The odorants used in the behavioral task. Names, purity and molecular structures of all odorants that were used in this study are shown.

steadily with increasing number of background odorants for both groups, yet several differences were evident. Mice trained to detect tiglate targets did worse on the task overall (mean \pm 95% confidence interval: $89.7 \pm 0.4\%$ and $92.4 \pm 0.5\%$ correct, respectively; $P < 10^{-10}$, two-proportion z -test) and were more affected by the number of components in the mixture than mice trained to detect non-tiglate targets (performance reduction of $0.82 \pm 0.06\%$ and $0.6 \pm 0.08\%$ per added odorant, respectively, mean \pm 95% confidence interval; $P < 0.01$). This difference is likely to be due to the greater similarity of tiglate odorants as a group, acting as better distractors or masks when the target is also a tiglate.

We further tested this hypothesis by analyzing how the presence of members of the two groups in the mixture affected behavioral performance. We used NoGo trials for further analysis of behavioral performance because $>90\%$ of incorrect responses were due to false alarms (Fig. 4a,b). We calculated the performance of mice detecting tiglates and mice detecting non-tiglates for all combinations of

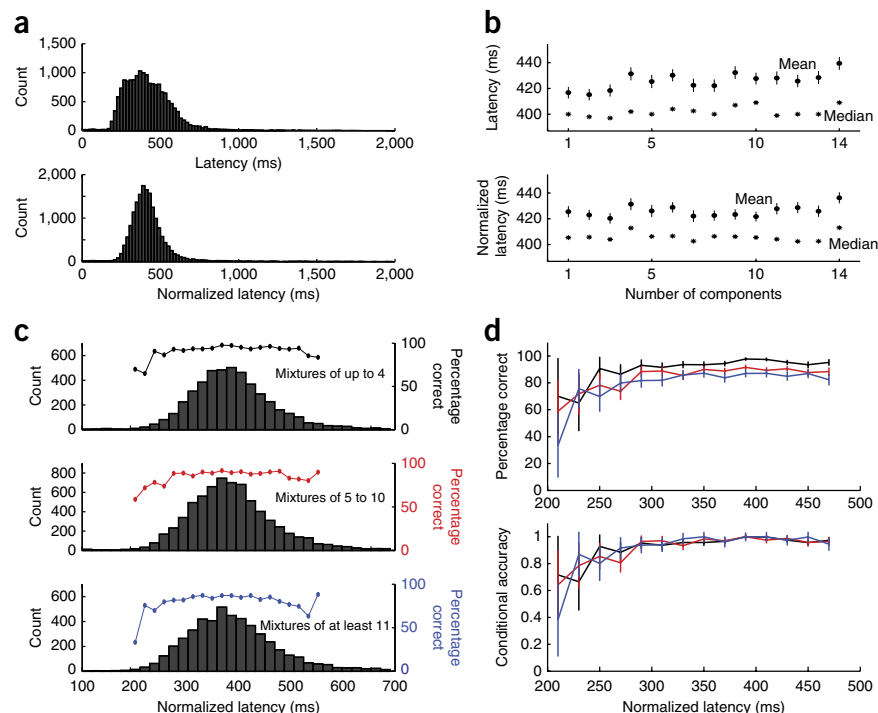
the numbers of tiglates and non-tiglates in the background mixture (Fig. 4c and d, respectively). The performance of mice detecting tiglate targets depended on the number of tiglate background odorants but was not affected much by non-tiglates (Fig. 4c). Conversely, the performance of mice detecting non-tiglate targets was independent of tiglate background but decreased as the number of non-tiglates increased (Fig. 4d). To quantify the effect of tiglates as background, we calculated the slopes of the rows in the matrices in Figure 4c,d, which allowed us to assess performance as a function of the number of tiglates in the background for a given number of non-tiglates (Fig. 4c,d, bottom). Similarly, we used the slopes of the columns of these matrices to quantify the effect of non-tiglates as background odorants (Fig. 4c,d, right). In an analysis of the distributions of these slopes for tiglate (Fig. 4e) and non-tiglate targets (Fig. 4f), the performance of mice detecting tiglate targets decreased by an average of $3.4 \pm 0.4\%$ for each added background tiglate but was unaffected by additional non-tiglates ($+0.4 \pm 0.5\%$; the two slopes are significantly different, $P = 1.6 \times 10^{-4}$, Mann-Whitney U -test). Conversely the performance of mice detecting non-tiglate targets decreased by an average of $2.7 \pm 0.5\%$ for each non-tiglate added to the background but was unaffected by background tiglates ($0.0 \pm 0.5\%$; slope difference significant, $P = 1.9 \times 10^{-4}$, Mann-Whitney U -test). We found a similar dependence between the group effect of background odorants and the target when analyzing the behavior of individual mice separately (Supplementary Fig. 4). The uncertain relationship between chemical similarity of odorants and the corresponding perceptual similarity³² raises the question of whether other groupings may also show a strong behavioral effect. We repeated the analysis of group effect as done for tiglates and non-tiglates, this time with all 12,870 possible divisions of the 16 odorants into two groups of 8, treating separately the data from mice detecting tiglate targets (Fig. 4g) and non-tiglate targets (Fig. 4h). Notably, tiglates were among the 2nd percentile of groups with the strongest negative effect for mice detecting tiglates. Analyzing the 50 groups with the strongest effects, we found that tiglates were very common members of these groups for mice trained to detect tiglates (Fig. 4i, $P = 0.02$, Mann-Whitney U -test of fraction member for tiglates versus non-tiglates) but not for mice trained to detect non-tiglates (Fig. 4j, $P = 0.39$).

Glomerular activity patterns

The analysis described above was based on the similarity of functional groups between the odorants. However, the fact that two odorants contain a similar functional group does not necessarily imply that they are similar from the perspective of the nose. To obtain an independent physiological measure of the similarity between the odorants, we imaged glomerular responses to all odorants on the dorsal surface of the olfactory bulb^{33–37}. Glomerular input activity directly reflects the olfactory receptors that are activated by the odorants, and previous studies have found a correlation between the similarity of glomerular response patterns and the difficulty of discrimination²⁹. Naive anesthetized mice were used for these experiments to measure the similarity and overlap of odorant representations before training.

We measured odor-evoked responses in mice expressing the genetically encoded calcium indicator GCaMP3 in olfactory receptor neurons (Fig. 5a)³⁸. Example responses from the individual glomeruli from one experiment are shown in Figure 5b–d. The response to each odorant was represented as a vector of glomerular activity and the cross-correlation between these vectors was used as a measure of response similarity between pairs of odorants (Fig. 5d,e). When pooling all pairwise correlations from 6 experiments, tiglate to tiglate correlations (correlation coefficient = 0.49 ± 0.02 , $n = 168$) were

Figure 3 Decreased performance on mixtures with more odorant components is not explained by a limited sampling time. **(a)** The distribution of response latencies (top) and session-normalized response latencies (bottom; see Online Methods). **(b)** Response latency (top) and normalized response latency (bottom) as a function of the number of components in the mixture. Shown are mean \pm s.e.m. (•) and median (*). **(c)** Normalized latency distributions for mixtures of up to 4 odorants (top), 5 to 10 odorants (middle) and more than 10 odorants (bottom). The curves show the percentage of correct responses as a function of normalized latency for the three mixture ranges. **(d)** The curves from **c**, superimposed without scaling (top) and after scaling (bottom). Symbols show the mean and error bars show a 95% confidence interval.



higher than both non-tiglate to non-tiglate ($r = 0.43 \pm 0.02$, $n = 168$, $P = 0.016$, Kolmogorov-Smirnov test, $ks = 0.17$) and tiglate to non-tiglate correlations (correlation coefficient = 0.45 ± 0.01 , $n = 384$, $P = 0.004$, Kolmogorov-Smirnov test, $ks = 0.16$, Fig. 5f,g). Although the difference between the correlation distributions was significant, these distributions were highly overlapping and therefore could not fully explain the behavioral dependence on the odorant groups. Furthermore, comparison of the pairwise correlations within individual subjects revealed significant similarity of tiglates in only two of the six experiments. Nevertheless, to assess the significance of the division of the odorants into groups based on the tiglate functional group, we repeated the same analysis for all possible divisions of the 16 odorant pool into two groups of 8. For each group, we calculated the distribution of response correlations within the group and across groups. The separability of each group was measured by the Kolmogorov-Smirnov distance between these distributions (see Online Methods). Only 6% of odorant groups were more separable than tiglates (Fig. 5h). Taken together with the analysis of the behavioral data, these results indicate that the difficulty of figure-ground segregation in olfaction cannot be fully explained by the similarity between the representations of figure and background components at the level of olfactory bulb inputs.

Glomerular map overlap predicts performance

The decline in performance with increased similarity between the target and background components can be explained either as reflecting a decreased sensitivity to the target or as reflecting a perceived similarity of the mixture to the target. Owing to the asymmetry of the task (mice were rewarded for hits but not for correct rejections), mice can be expected to lick both when they sense the target (or think they do) and when they realize that the target is masked and cannot be detected. We tested each of these hypotheses by asking whether behavioral performance correlated with the degree of masking of target-evoked glomerular responses by background mixtures or whether performance correlated with the similarity between target-evoked glomerular responses and mixture-evoked glomerular responses. We based our analysis on a simple model that estimates mixture responses on the basis of the responses to the individual components. Mixture responses can involve nonlinear interactions anywhere within the mouse brain and therefore difficult to predict. We made the simplest

assumption and modeled the mixture response at the level of glomerular inputs as a linear sum of the responses to the individual components^{17,31,34,39,40}. On the basis of the linear summation model, each mixture presented in a behavioral trial was assigned a 'masking' value and a 'similarity' value. Masking reflected the fraction of target-evoked activity that is covered by the mixture-evoked activity (Fig. 6a; see Online Methods). As a measure of similarity we used the correlation between the target-evoked response and the mixture-evoked response.

Analyzing all NoGo trials, we found that performance significantly degraded with increasing masking (Fig. 6b, correlation coefficient = 0.78 , $P = 4.7 \times 10^{-7}$, $n = 30$ 500-trial bins) but not with similarity (Fig. 6c, correlation coefficient = 0.36 , $P = 0.05$, $n = 30$ 500-trial bins). Although the increase in both masking and correlation was accompanied by an increase in the average number of mixture components (Fig. 6d,e), similar trends were evident even within a fixed number of components for both masking ($P < 0.01$ for mixtures of more than 3 components; Fig. 6f) and correlation ($P < 0.01$ for mixtures of more than 10 components; Fig. 6g). Of note, masking values of less than 0.7 had no effect on behavioral performance, suggesting redundancy in the coding of the target by multiple glomeruli. To ensure that the above results are not simply due to our assumption of linear summation of glomerular responses for mixture stimuli, we tested another model, which assumed no summation. Instead, this model assumed that the mixture response in each glomerulus is the maximum of the individual odorant responses (maximal intensity projection). We found a similar drop in performance with increased masking using the maximal intensity projection model as well (correlation coefficient = 0.68 , $P = 3.9 \times 10^{-5}$; Supplementary Fig. 5), indicating that this drop in performance with increased masking is not sensitive to the exact model of summation.

These data show that the behavioral difficulty of detecting a target odorant within a mixture is closely linked to the constraints of combinatorial coding by glomeruli in the olfactory bulb and not to similarity of the target and background mixtures. Mixtures components that are similar to the target act as powerful distractors not by making

Figure 4 Performance depends on background components that are similar to the target.

(a,b) Behavioral performance as a function of the number of background components for mice trained to detect tiglate targets (a) and mice trained to detect non-tiglate targets (b). Mean \pm 95% confidence interval are shown. (c,d) Behavioral performance as a function of the number of tiglats and non-tiglats in the background for mice trained to detect tiglate targets (c) and mice trained to detect non-tiglate targets (d). Bottom panels show linear fits to the rows of the colored matrices. Right panels show linear fits to the columns of the colored matrices. (e,f) The slopes of the linear fits from c,d, respectively. Blue and red arrows show the mean slope for tiglats and non-tiglats, respectively. (g,h) The distributions of the effects of all 12,780 possible 8-odorant groups on the performance of mice detecting tiglats (g) and mice detecting non-tiglats (h). Blue and red arrows mark the group effects of tiglats and non-tiglats, respectively, obtained from e and f. (i,j) The composition of the 50 groups that had the strongest negative effects on performance of mice detecting tiglate targets (i) and mice detecting non-tiglate targets (j). The bar for each odorant shows the fraction of the 50 groups in which it was a member.

the mixture more similar to the target, but by masking target-evoked activity.

DISCUSSION

We analyzed quantitatively the behavioral ability of mice to detect odorants of interest in the presence of variable backgrounds, a feature that is probably fundamental to the survival of many species. Our main findings are that (i) mice are highly capable of performing such a task, (ii) similarity between mixture components and the target odorant determines the difficulty of the task, and (iii) the difficulty of the task depends on the extent to which background odorants and the target odorants overlap in the glomerular activity patterns they elicit. Presumably, the last two findings are related because it is likely that inclusion of background odorants that are similar to the target increases the extent of glomerular activity overlap.

Our finding that mice can detect the presence (or absence) of the target when mixtures with many components are presented is in contrast with the common view of olfaction as a synthetic sense wherein mixtures of odorants are perceived as a whole rather than being analyzed to detect and identify their components^{8–11,19–23}. This view largely relies on the observation that humans are very poor at analyzing mixtures or even detecting target odorants within mixtures^{8–10}. Studies using rodents also inferred poor detection of single odorants within mixtures, but these were based on either spontaneous unrewarded discrimination²¹ or an assumption that animals generalize task rules¹⁹. The data presented here indicate that macroscopic mammals can detect single odorants within mixtures. In fact, anecdotal data have already shown that rats can discriminate between two mixtures of ten odorants that differ by only one component²⁴. While

demonstrating strong analytical abilities, our data should not be taken as evidence against synthesis in olfaction. It is possible that the olfactory system has both analytic and synthetic abilities, allowing both grouping of odorants into objects and differentiation between objects. Whether a specific odorant should be searched for in a mixture or whether it should be synthetically combined with other odorants to identify an object may require learning of its behavioral relevance and may be context dependent.

We found that increasing the number of background components gradually and steadily decreased behavioral accuracy. A recent study found that the structure of stimulus presentation can greatly affect decision accuracy and that grouping trials of similar difficulty into blocks within behavioral sessions may increase behavioral accuracy by allowing a more accurate internal representation of the boundary between rewarded and unrewarded stimuli³⁰. Because trials of varying difficulties were interleaved in our experiments, it is possible

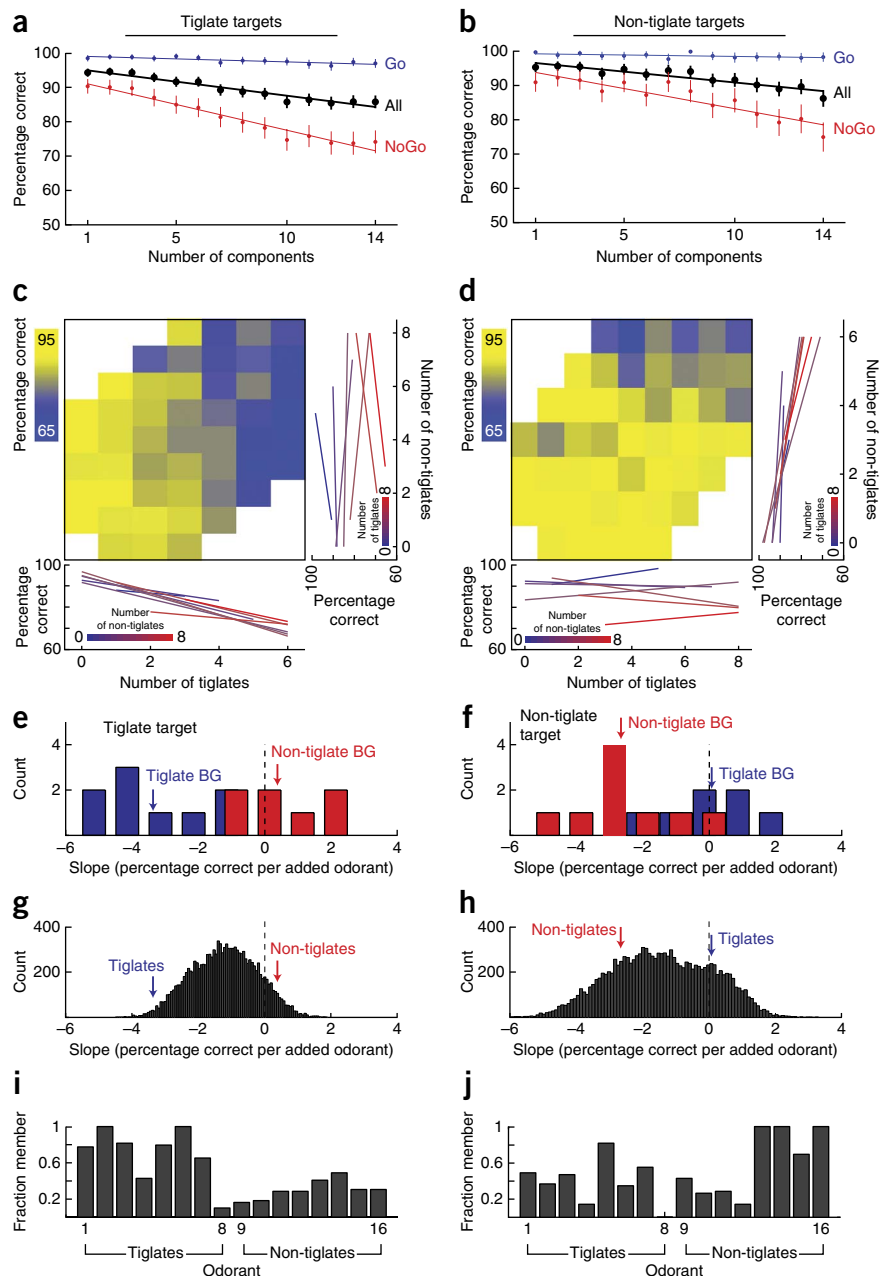
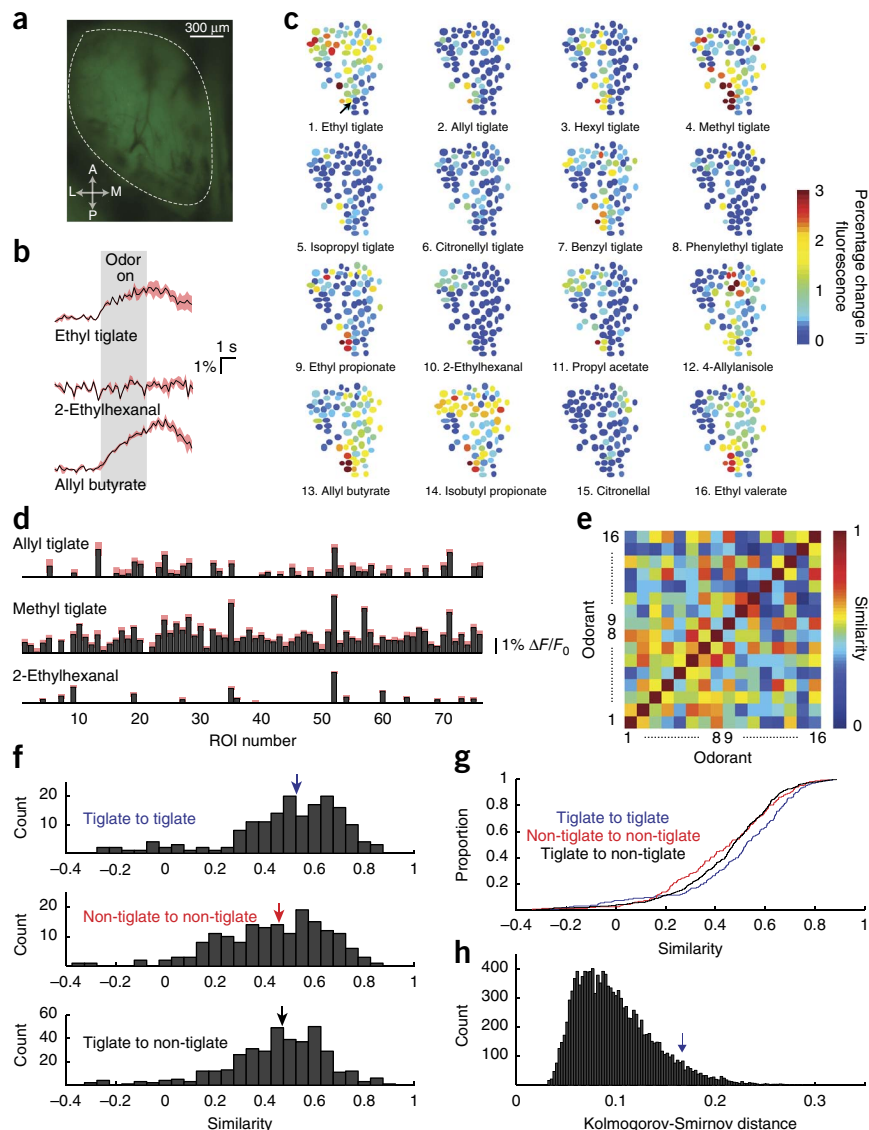


Figure 5 Tiglates evoke correlated glomerular response patterns. **(a)** Raw fluorescence image of the olfactory bulb of an OMP-GCaMP3 mouse with a typical imaged region highlighted (white dashed line). A, anterior; P, posterior; M, medial; L, lateral. **(b–e)** Analysis of the responses recorded from one mouse. **(b)** The time course of the responses in the glomerulus marked by an arrow in top left panel of **c** to three odorants. The mean response is shown in black and the s.e.m. in red ($n = 5$ repetitions). **(c)** Glomerular response patterns elicited by each of the 16 odorants. Putative glomeruli were selected as regions of interest (ROIs) and the response magnitude for each ROI is color coded. Odorants 1 to 8 are tiglates. **(d)** The responses of all glomeruli to three odorants represented as response vectors. Mean responses are shown in gray and the s.e.m. in red ($n = 5$ repetitions). **(e)** The correlation matrix of the odorant responses shown in **b**. Tiglate to tiglate correlations are shown in the bottom left quadrant (odorants 1 to 8). **(f)** The distribution of correlation coefficients for tiglate to tiglate (top), non-tiglate to non-tiglate (middle) and tiglate to non-tiglate (bottom). Data are pooled from all experiments ($n = 6$). Colored arrows in each plot show the distribution median. **(g)** The same distributions as in **f** plotted as cumulative distributions to promote visualization of the differences. **(h)** The separability of all 12,870 possible groups of 8 odorants as measured by Kolmogorov-Smirnov distance between the distributions of correlation coefficients within a group and across groups. Blue arrow denotes the Kolmogorov-Smirnov distance between tiglate to tiglate correlations and tiglate to non-tiglate correlations.



that mice can perform even better in more predictable conditions.

Our experimental design allowed us to dissect the features of background mixtures that affected detection of target odorants. We found that odorants that contain the functional group tiglate were strong maskers for targets that contained the same functional group but not for other targets. For the odorant pool used in this set of experiments, a common tiglate functional group was also accompanied by higher similarity of glomerular response patterns, yet this difference was too small to account for the behavioral effect. Taken together, these findings imply that not all odorants are equally potent as maskers and that the potency of any odorant is related to its similarity to the specific target it has to mask.

We used a simple model to estimate the glomerular response patterns elicited by all mixtures that were presented in the behavioral task. Using this model, we showed that performance can be explained by the extent to which mixtures evoke glomerular activity patterns that overlap with the target. Notably, similarity between mixture- and target-evoked activities does not explain behavioral performance. Glomerular response patterns were recorded from naive animals to represent the initial input signals the mice had to process during training. How exposure and learning-related changes in glomerular patterns^{41–43} contribute to performance on the task will be the subject of future studies.

Our model assumed no lateral interactions. While this has shown to be the case at the input stage^{17,31,34,39,40}, lateral interactions downstream

may certainly influence mixture analysis. Because odor-specific lateral interactions are not well characterized in the olfactory bulb of mammals, we chose to keep the model simple. An upper bound and a lower bound to mixture response estimates were obtained from linear model (Fig. 6) and a maximal projection intensity model (Supplementary Fig. 5), respectively. Both models reached similar conclusions. Future experiments will be directed at the mechanism by which the olfactory cocktail party problem is solved. Potential mechanisms include hard-wired strategies analogous to preattentive segmentation in the visual system⁴⁴. However, the fact that behavioral performance only degraded at high values of glomerular masking suggests that learning-related changes in either the olfactory bulb circuits or cortical circuits are involved^{45–47}. Additionally, cortico-bulbar feedback^{48,49} may enable flexible context-dependent classification of stimuli. A temporal jitter between odorant onset has been suggested to contribute to scene segmentation^{16,25,26}. In natural turbulent environments, covariance of components from a common source may similarly be instrumental for scene segmentation by providing the temporal jitter⁵⁰. Careful analysis of combined behavioral and physiological recordings will be critical to uncovering the mechanisms by which figure-ground segregation is achieved in the olfactory system.

Figure 6 Performance on the task depends on masking at the level of olfactory bulb inputs.

(a) Estimation of the masking of target inputs to the olfactory bulb by a background mixture (left) and of the correlation between target and mixture inputs (right). Mixture responses are modeled as the linear sum of the responses to the individual components. Masking (bounded between 0 and 1) is calculated for each target-activated glomerulus, and the masking of all glomeruli is then averaged to obtain the mixture masking value. Grayscale levels in the cartoon glomeruli denote activity level. (b,c) Percentage of NoGo trials that were correctly rejected as a function of target masking (b) and target-mixture correlation (c). Data were grouped in 500-trial bins. Red lines are fits of a logistic sigmoidal decay to the data (see Online Methods). Below are the distributions of masking and correlation values for all mixtures presented in NoGo trials. (d,e) Average number of components in the mixture as a function of mixture masking (d) and target-mixture correlation (e). (f,g) Percentage of NoGo trials with fixed number of components in the mixture that were correctly rejected as a function of target masking (f) and target-mixture correlation (g). Each curve shows the data from a fixed number of components in the mixture (indicated by color; BG represents the number of components in the background mixture). Black lines are fits of a logistic sigmoidal decay to the data (see Online Methods).

METHODS

Methods and any associated references are available in the [online version of the paper](#).

Note: Any Supplementary Information and Source Data files are available in the [online version of the paper](#).

ACKNOWLEDGMENTS

We thank N. Uchida, R. Wilson and members of our laboratory for comments on the manuscript. Work in V.N.M.'s laboratory was supported by grants from the US National Institutes of Health (RO1DC11291). D.R. was supported by a fellowship from the Edmond and Lily Safra Center for Brain Sciences, Hebrew University.

AUTHOR CONTRIBUTIONS

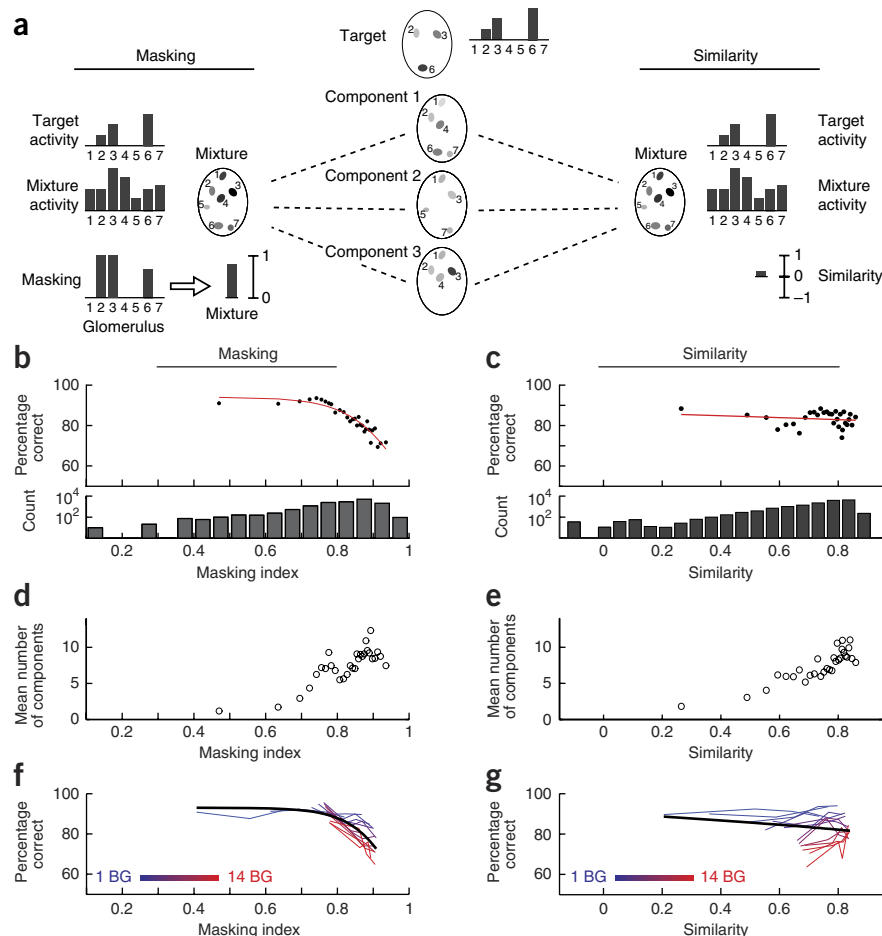
D.R. and V.N.M. conceived and designed the experiments. D.R. and V.H. collected the behavioral data. V.K. collected the imaging data. D.R. analyzed the behavioral data. D.R. and V.K. analyzed the imaging data. D.R. and V.N.M. wrote the manuscript.

COMPETING FINANCIAL INTERESTS

The authors declare no competing financial interests.

Reprints and permissions information is available online at <http://www.nature.com/reprints/index.html>.

1. Apfelbach, R., Blanchard, C.D., Blanchard, R.J., Hayes, R.A. & McGregor, I.S. The effects of predator odors in mammalian prey species: a review of field and laboratory studies. *Neurosci. Biobehav. Rev.* **29**, 1123–1144 (2005).
2. Howard, W.E., Marsh, R.E. & Cole, R.E. Food detection by deer mice using olfactory rather than visual cues. *Anim. Behav.* **16**, 13–17 (1968).
3. Blaustein, A.R. Sexual selection and mammalian olfaction. *Am. Nat.* **117**, 1006–1010 (1981).
4. Crouzet, S.M. & Serre, T. What are the visual features underlying rapid object recognition? *Front. Psychol.* **2**, 326 (2011).
5. Wolfson, S.S. & Landy, M.S. Examining edge- and region-based texture analysis mechanisms. *Vision Res.* **38**, 439–446 (1998).
6. Elhilali, M. & Shamma, S.A. A cocktail party with a cortical twist: how cortical mechanisms contribute to sound segregation. *J. Acoust. Soc. Am.* **124**, 3751–3771 (2008).



7. McDermott, J.H. The cocktail party problem. *Curr. Biol.* **19**, R1024–R1027 (2009).
8. Jinks, A. & Laing, D.G. A limit in the processing of components in odour mixtures. *Perception* **28**, 395–404 (1999).
9. Laing, D.G. & Francis, G.W. The capacity of humans to identify odors in mixtures. *Physiol. Behav.* **46**, 809–814 (1989).
10. Jinks, A. & Laing, D.G. The analysis of odor mixtures by humans: evidence for a configurational process. *Physiol. Behav.* **72**, 51–63 (2001).
11. Wilson, D.A. & Stevenson, R.J. Olfactory perceptual learning: the critical role of memory in odor discrimination. *Neurosci. Biobehav. Rev.* **27**, 307–328 (2003).
12. Hopfield, J.J. Odor space and olfactory processing: collective algorithms and neural implementation. *Proc. Natl. Acad. Sci. USA* **96**, 12506–12511 (1999).
13. Polak, E.H. Multiple profile-multiple receptor site model for vertebrate olfaction. *J. Theor. Biol.* **40**, 469–484 (1973).
14. Koulakov, A., Gelperin, A. & Rinberg, D. Olfactory coding with all-or-nothing glomeruli. *J. Neurophysiol.* **98**, 3134–3142 (2007).
15. Giraudet, P., Berthommier, F. & Chaput, M. Mitral cell temporal response patterns evoked by odor mixtures in the rat olfactory bulb. *J. Neurophysiol.* **88**, 829–838 (2002).
16. Shen, K., Tootoonian, S. & Laurent, G. Encoding of mixtures in a simple olfactory system. *Neuron* **10.1016/j.neuron.2013.08.026** (2013).
17. Tabor, R., Yaksi, E., Weislogel, J.-M. & Friedrich, R.W. Processing of odor mixtures in the zebrafish olfactory bulb. *J. Neurosci.* **24**, 6611–6620 (2004).
18. Arnson, H.A. & Holy, T.E. Robust encoding of stimulus identity and concentration in the accessory olfactory system. *J. Neurosci.* **33**, 13388–13397 (2013).
19. Frederick, D.E., Barlas, L., Levins, A. & Kay, L.M. A critical test of the overlap hypothesis for odor mixture perception. *Behav. Neurosci.* **123**, 430–437 (2009).
20. Laska, M. & Hudson, R. Discriminating parts from the whole: determinants of odor mixture perception in squirrel monkeys, *Saimiri sciureus*. *J. Comp. Physiol. A* **173**, 249–256 (1993).
21. Wiltout, C., Dogra, S. & Linster, C. Configurational and nonconfigurational interactions between odorants in binary mixtures. *Behav. Neurosci.* **117**, 236–245 (2003).
22. Kay, L.M., Crk, T. & Thorngate, J. A redefinition of odor mixture quality. *Behav. Neurosci.* **119**, 726–733 (2005).
23. Wilson, D.A. Pattern separation and completion in olfaction. *Ann. NY Acad. Sci.* **1170**, 306–312 (2009).
24. Barnes, D.C., Hofacer, R.D., Zaman, A.R., Rennaker, R.L. & Wilson, D.A. Olfactory perceptual stability and discrimination. *Nat. Neurosci.* **11**, 1378–1380 (2008).

25. Linster, C., Henry, L., Kadohisa, M. & Wilson, D.A. Synaptic adaptation and odor-background segmentation. *Neurobiol. Learn. Mem.* **87**, 352–360 (2007).
26. Saha, D. *et al.* A spatiotemporal coding mechanism for background-invariant odor recognition. *Nat. Neurosci.* **16**, 1830–1839 (2013).
27. Abraham, N.M. *et al.* Maintaining accuracy at the expense of speed: stimulus similarity defines odor discrimination time in mice. *Neuron* **44**, 865–876 (2004).
28. Rinberg, D., Koulakov, A. & Gelperin, A. Speed-accuracy tradeoff in olfaction. *Neuron* **51**, 351–358 (2006).
29. Uchida, N. & Mainen, Z.F. Speed and accuracy of olfactory discrimination in the rat. *Nat. Neurosci.* **6**, 1224–1229 (2003).
30. Zariwala, H.A., Kepecs, A., Uchida, N., Hirokawa, J. & Mainen, Z.F. The limits of deliberation in a perceptual decision task. *Neuron* **78**, 339–351 (2013).
31. Grossman, K.J., Mallik, A.K., Ross, J., Kay, L.M. & Issa, N.P. Glomerular activation patterns and the perception of odor mixtures. *Eur. J. Neurosci.* **27**, 2676–2685 (2008).
32. Segundo, L., Snitz, K. & Sobel, N. The perceptual logic of smell. *Curr. Opin. Neurobiol.* **25**, 107–115 (2014).
33. Ma, L. *et al.* Distributed representation of chemical features and tunotopic organization of glomeruli in the mouse olfactory bulb. *Proc. Natl. Acad. Sci. USA* **109**, 5481–5486 (2012).
34. McGann, J.P. *et al.* Odorant representations are modulated by intra- but not interglomerular presynaptic inhibition of olfactory sensory neurons. *Neuron* **48**, 1039–1053 (2005).
35. Meister, M. & Bonhoeffer, T. Tuning and topography in an odor map on the rat olfactory bulb. *J. Neurosci.* **21**, 1351–1360 (2001).
36. Soucy, E.R., Albeanu, D.F., Fantana, A.L., Murthy, V.N. & Meister, M. Precision and diversity in an odor map on the olfactory bulb. *Nat. Neurosci.* **12**, 210–220 (2009).
37. Uchida, N., Takahashi, Y.K., Tanifuji, M. & Mori, K. Odor maps in the mammalian olfactory bulb: domain organization and odorant structural features. *Nat. Neurosci.* **3**, 1035–1043 (2000).
38. Isogai, Y. *et al.* Molecular organization of vomeronasal chemoreception. *Nature* **478**, 241–245 (2011).
39. Fletcher, M.L. Analytical processing of binary mixture information by olfactory bulb glomeruli. *PLoS ONE* **6**, e29360 (2011).
40. Lin, D.Y., Shea, S.D. & Katz, L.C. Representation of natural stimuli in the rodent main olfactory bulb. *Neuron* **50**, 937–949 (2006).
41. Kass, M.D., Moberly, A.H., Rosenthal, M.C., Guang, S.A. & McGann, J.P. Odor-specific, olfactory marker protein-mediated sparsening of primary olfactory input to the brain after odor exposure. *J. Neurosci.* **33**, 6594–6602 (2013).
42. Abraham, N.M., Vincis, R., Lagier, S., Rodriguez, I. & Carleton, A. Long term functional plasticity of sensory inputs mediated by olfactory learning. *Elife* **3**, e02109 (2014).
43. Jones, S.V., Choi, D.C., Davis, M. & Ressler, K.J. Learning-dependent structural plasticity in the adult olfactory pathway. *J. Neurosci.* **28**, 13106–13111 (2008).
44. Treisman, A.M. & Gelade, G. A feature-integration theory of attention. *Cognit. Psychol.* **12**, 97–136 (1980).
45. Chappuis, J. & Wilson, D.A. Bidirectional plasticity of cortical pattern recognition and behavioral sensory acuity. *Nat. Neurosci.* **15**, 155–161 (2012).
46. Choi, G.B. *et al.* Driving opposing behaviors with ensembles of piriform neurons. *Cell* **146**, 1004–1015 (2011).
47. Haberly, L.B. Parallel-distributed processing in olfactory cortex: new insights from morphological and physiological analysis of neuronal circuitry. *Chem. Senses* **26**, 551–576 (2001).
48. Boyd, A.M., Sturgill, J.F., Poo, C. & Isaacson, J.S. Cortical feedback control of olfactory bulb circuits. *Neuron* **76**, 1161–1174 (2012).
49. Markopoulos, F., Rokni, D., Gire, D.H. & Murthy, V.N. Functional properties of cortical feedback projections to the olfactory bulb. *Neuron* **76**, 1175–1188 (2012).
50. Brody, C.D. & Hopfield, J.J. Simple networks for spike-timing-based computation, with application to olfactory processing. *Neuron* **37**, 843–852 (2003).

ONLINE METHODS

All experimental procedures were performed using approved protocols in accordance with institutional (Harvard University IACUC) and national guidelines.

Behavior. Subjects and surgery. Thirteen c57bl6 adult male mice (Charles River) were trained on the behavioral task. No statistical methods were used to predetermine sample sizes, but our sample sizes are similar to those reported in previous publications^{27–29}. Mice were first anesthetized (ketamine and xylazine, 100 and 10 mg/kg, respectively) and a metal plate was attached to their skull with dental acrylic for subsequent head restraint. Mice were then maintained in a reversed light/dark cycle facility. All behavioral training and testing was done during the subjective night time.

Apparatus. The behavioral apparatus was located inside a sound-attenuating box (Med Associates, VT, USA) and consisted of a head restraining device, an odor delivery system, a lick detector and a water delivery system. Odor delivery, monitoring of licking and water rewards were controlled using computer interface hardware (National Instruments) and custom software written in LabView. The mouse was continuously monitored using a CCD camera during behavior sessions.

Mixture presentation. Odorant mixtures were presented using a custom-made olfactometer that was designed to have constant flow (2.5 l/min) and to have the concentrations of the different odorants independent of each other (Supplementary Fig. 1). The olfactometer was composed of 16 odor modules. Each module was made of two glass tubes, one containing the odor and one containing only the odor solvent. A three-way valve (Lee Company, USA) diverted an input flow of filtered air to either the odor tube or the solvent tube, and the output of the two tubes was merged to form the module output. This design ensured that each module contributed a constant amount of flow at any time. Input flow to the modules and output flow from the modules were made through FEP-lined Tygon/PVC tubing connected in symmetric pairwise bifurcations to ensure equal flow through all modules. All odorants were diluted to 2% v/v in diethyl phthalate in the tubes and then further diluted by the flow of other modules 16-fold. The odorant mixture was carried from the point of final odorant convergence to the odor port through a 4-foot length of tubing with an inner diameter of 1/16 inch to allow mixing while minimizing the latency from valve opening to odor presentation at the mouse's nostrils. Olfactometer output was analyzed with a photoionization detector (miniPID, Aurora Scientific) to test for latency (170 ms), repeatability (mean coefficient of variation, $6 \pm 0.8\%$), and independence of the modules (see Supplementary Fig. 1).

Behavioral training and testing. After 1 week of recovery from surgery to implant headplates, mice were water deprived. Mice were acclimatized to the behavioral apparatus for 2 d in which they were allowed 30 min of free exploration with water freely available at the water port. This was followed by an additional day in which they were head restrained and were allowed water freely from the port. After acclimatization, mice were trained on the behavioral task. No randomized process was used to assign target odorants to each mouse. A mixture was presented for 2 s every 10 s and mice had to respond correctly within the 2-s period. Correct licks were rewarded with a 10- μ l water drop, correct rejections were not rewarded, and incorrect trials were punished by a 5-s timeout. Training began with easy sessions and, as mice reached 80% performance over a whole session, session difficulty was adjusted. The difficulty of the task was controlled by varying the distribution of the number of components in the mixture using the following equation:

$$p(x) = \frac{b^x}{\sum_{i=1}^{14} b^i}$$

where $p(x)$ is the probability of x components (ranging from 1 to 14). The parameter b was first set to 0.25 and was raised in increments of 0.25 when the mouse reached a performance of 80% correct until reaching $b = 1$. This allowed varying task difficulty without any changes in task rules. The number of training sessions varied across mice, ranging from 4 to 19, with an average and s.d. of 9.2 ± 5 sessions. Unless specified otherwise, all data presented were taken from sessions with flat distributions of the number of components in the mixture ($b = 1$). Mice performed one session per day with an average of 346 ± 90 trials per session (lasting typically about an hour), and each mouse performed between 4 and

10 test sessions (6.7 ± 1.8 , mean \pm s.d.). Data collection and analysis were not performed blind to the conditions of the experiments.

Odor set. Since odorant space is not easily parameterized and defined^{32,51}, a complete analysis of the behavioral capacity is impossible, and odorant choice may affect the conclusions from behavioral experiments. We chose the odorants to be used in the task with two goals in mind: (i) making the task difficult, to allow failures in performance, and (ii) having variable similarities between odorants to study the dependence of difficulty of figure-ground segregation on figure-ground similarity. With the difficulty of defining odorant similarity, we settled on 8 odorants from the tiglate family and 8 other odorants (non-tiglates) for the task (Fig. 2).

Odorants were obtained from Sigma Aldrich (ethyl tiglate, allyl tiglate, hexyl tiglate, methyl tiglate, isopropyl tiglate, ethyl propionate, 2-ethylhexanal, 4-allylanisole, (\pm)citronellal, isobutyl propionate, allyl butyrate, propyl acetate), Penta (benzyl tiglate, phenylethyl tiglate, citronellyl tiglate) and Alfa Aesar (ethyl valerate). The target odorant pairs and the number of mice trained to detect each pair are as follows: ethyl tiglate and allyl tiglate, two mice. Hexyl tiglate and methyl tiglate, one mouse. Isopropyl tiglate and citronellyl tiglate, one mouse. Benzyl tiglate and phenylethyl tiglate, four mice. Ethylpropionate and 2-ethylhexanal, one mouse. Propyl acetate and 4-allylanisole, one mouse. Ethylvalerate and citronellal, two mice. Isobutyl propionate and allyl butyrate, one mouse.

Data analysis. (i) Latency measurement. Latency was defined as the time from odor valve opening to lick detection. Per photoionization detector measurements, 170 ms were taken off all latency values to account for the time it took for the odor to travel from the valve to the mouse nose. To remove intersession variability in response latencies that most likely reflected variability in the positioning of the water port, latency values were normalized to the mean value of their corresponding session. Values (between 0 and 1) were then multiplied by the mean of all trials from all sessions to obtain values that could be compared to the un-normalized values. Data distribution (shown in Fig. 3) was assumed to be normal, but this was not formally tested. (ii) Analysis of odorant group effects on behavior (Fig. 4). To estimate the effect of tiglates as a group on behavioral performance, we plotted the percent of correct rejections as a function of the number of background tiglates while holding the number of non-tiglates constant. This was done for all numbers of non-tiglates, yielding 9 such curves (0 to 8 non-tiglate background odorants). Linear fits were made to all 9 curves and the average slope of these curves was taken to be the group effect of the tiglates. The same analysis was repeated for other groups of 8 odorants within the 16-odorant pool.

Imaging. Experimental procedure. Adult OMP-GCaMP3 mice³⁸ were anesthetized with ketamine and xylazine (100 and 10 mg/kg, respectively) and the cranial bones over the olfactory bulbs were thinned with a dental drill to allow clear visualization. Two photo lenses coupled front to front were used to image the olfactory bulb surface onto the sensor of a CMOS camera (DFK 23GPO31, The Imaging Source GmbH). Images (640 \times 480 pixels) were acquired at 8-bit resolution and 4–6 frames/s. Data from the camera were recorded to the computer via data acquisition hardware (National Instruments). A blue LED (CBT-90, Luminus, Billerica, Massachusetts) coupled to an optical fiber was used for excitation.

All odorants were diluted to 5% v/v in diethyl phthalate and were delivered using an automated olfactometer³⁶. The 16 odors and an additional tube containing only diethyl phthalate were presented in random order, and each odor was repeated 3–5 times. Odors were presented every 45 s for 3 s, with data acquisition beginning 3 s before and ending 3 s after odor presentation.

Data analysis. The acquired sequence of images was converted to $\Delta F/F_0$ images (change in fluorescence/resting fluorescence). We then calculated the maximal response at each pixel for all 16 odorants. These maximum response maps were used to identify putative glomeruli as regions of interest (ROIs) for further analysis (ranging from 55 to 76 ROIs per experiment). The response at each ROI was quantified by integrating the $\Delta F/F_0$ signal during odor presentation. This procedure yielded responses that were represented as response vectors in a space that is defined by the ROIs.

(i) Analysis of glomerular map similarity. To quantify the similarity between the activity patterns of different odors, we calculated the cross-correlation between the response vectors of pairs of odors. We analyzed the separability of odorant groups by calculating the Kolmogorov-Smirnov distances between the distributions of correlation coefficients within a group and across groups. A high Kolmogorov-Smirnov distance would mean that the similarity among



members of the group is higher than the similarity between members of the group and other odorants.

(ii) Analysis of mixture masking and similarity to target. Two models were used to estimate the extent to which a mixture masks the target at the level of olfactory bulb glomeruli: a linear model and a maximal intensity projection model. Both models assumed that there are no lateral interactions between glomeruli at the level of inputs. The first model assumed linear summation at each glomerulus to obtain an upper bound to the mixture response: that is, the response to a mixture would be the exact linear sum of the responses to the components. The second model provided an alternative for deriving mixture responses and assumed no summation. The response to a mixture at each glomerulus was taken to be the maximum of the responses at that glomerulus to the mixture components.

Masking at each target-activated glomerulus was calculated using the following equation:

$$M_i(m, T) = \begin{cases} \frac{a_i(m)}{a_i(T)}, & 0 < \frac{a_i(m)}{a_i(T)} < 1 \\ 0, & \frac{a_i(m)}{a_i(T)} < 0 \\ 1, & \frac{a_i(m)}{a_i(T)} > 1 \end{cases}$$

where $M_i(m, T)$ is the masking of target T by mixture m at the i^{th} glomerulus, and $a_i(m)$ and $a_i(T)$ are the responses of the i^{th} glomerulus to mixture m and target T , respectively. Only glomeruli that were activated by the target above threshold (3 s.d. away from the baseline) were considered for this analysis to avoid divergence due to small denominators (see **Supplementary Fig. 6** for a test of robustness).

The masking value for the mixture was then taken to be the average masking of all target-activated glomeruli:

$$M(m, T) = \frac{1}{N} \sum_{i=1}^N M_i(m, T)$$

where $M(m, T)$ is the masking of target T by mixture m and N is the number of target-activated glomeruli. Glomeruli that were not activated by the target were not considered for this analysis. Masking values were calculated for the two targets and the larger of these was taken to be the mixture's masking value, with the assumption that it is enough to mask one target to preclude the mouse from being able to make a decision. The relationship between the masking index and behavioral performance was quantified by first binning trials according to their masking index and plotting the mean performance in each bin against the mean masking index. A decaying logistic function was fit to these data:

$$a \left(1 - \frac{1}{1 + e^{-sM + b}} \right)$$

where a is the saturated performance and s and b determine the slope of the decay and the shift along the masking axis. M is the masking index value.

The similarity to the target was calculated for each mixture as the cross-correlation between the target and the mixture response vectors. The relationship between the target-mixture similarity and behavioral performance was quantified in the same way as for masking.

51. Koulakov, A.A. & Rinberg, D. In search of the structure of human olfactory space. *Front. Syst. Neurosci.* **5**, 65 (2011).